

1 **Historical reconstruction of Ocean Acidification in the Australian region**

2

3 Andrew Lenton¹

4 Bronte Tilbrook^{1,2}

5 Richard J. Matear¹

6 Tristan P. Sasse³

7 Yukihiro Nojiri⁴

8

9 ¹CSIRO Oceans and Atmosphere, Hobart, Australia

10 ²Antarctic Climate and Ecosystems Co-operative Research Centre, Hobart, Australia

11 ³Climate Change Research Centre, Kensington Campus, University of New South
12 Wales, Sydney, Australia

13 ⁴National Institute for Environmental Studies, Tsukuba, Japan

14

15 **1. Abstract**

16 The ocean has become more acidic over the last 200 years in response increasing
17 atmospheric carbon dioxide (CO₂) levels. Documenting how the ocean has changed is
18 critical for assessing how these changes impact marine ecosystems, and for the
19 management of marine resources. Here we use present day ocean carbon
20 observations, from shelf and offshore waters around Australia, combined with neural
21 network mapping of CO₂, sea surface temperature and salinity to estimate the current
22 seasonal and regional distributions of carbonate chemistry (pH and aragonite
23 saturation state). The observed changes in atmospheric CO₂ and SST and
24 climatological salinity are then used to reconstruct pH and aragonite saturation state
25 changes over the last 140 years (1870–2013). The comparison with data collected at
26 Integrated Marine Observing System National Reference Station sites located on the
27 shelf around Australia shows that both the mean state, and seasonality in the present
28 day are well represented, with the exception of sites such as the Great Barrier Reef.
29 Our reconstruction predicts that since 1870 an average decrease in aragonite
30 saturation state of 0.48 and of 0.09 in pH has occurred in response to increasing
31 oceanic uptake of atmospheric CO₂. Large seasonal variability in pH and aragonite
32 saturation state occur in Southwestern Australia driven by ocean dynamics (mixing)
33 and in the Tasman Sea by seasonal warming (in the case of aragonite saturation state).

34 The seasonal and historical changes in aragonite saturation state and pH have different
35 spatial patterns and suggest that the biological responses to ocean acidification are
36 likely to be non-uniform depending on the relative sensitivity of organisms to shifts in
37 pH and saturation state. This new historical reconstruction provides an important link
38 to biological observations that will help to elucidate the consequences of ocean
39 acidification.

40

41 **2. Introduction**

42 The ocean plays a key role in reducing the rate of global climate change, absorbing
43 approximately 30% of the anthropogenic CO₂ emitted over the last 200 years (Ciais et
44 al., 2013), and more than 25% of current CO₂ emissions (Le Quéré, 2015). The CO₂
45 taken up by the ocean reacts in seawater, leading to decreases in pH and dissolved
46 carbonate ion concentrations (CO₃²⁻), these changes being collectively referred to as
47 ocean acidification. Over the past 200 years, it is estimated that there has been a 0.1
48 unit reduction in the ocean's surface pH, or 26% increase in the concentration of
49 hydrogen ion concentrations in seawater (Doney et al., 2009).

50

51 Current projections suggest that the increase in hydrogen ion concentration is likely to
52 be greater than 100% (than the preindustrial period) by the end of the century under
53 high emissions trajectories e.g. Matear and Lenton (2014). Furthermore these changes
54 will persist for many millennia e.g. Frolicher and Joos (2010). Ocean acidification is
55 likely to impact the entire marine ecosystem - from microbial communities to top
56 predators. Factors that can be impacted include reproductive health, organism growth
57 and physiology, species composition and distributions, food web structure and
58 nutrient availability (Aze et al., 2014; Doney et al., 2012; Dore et al., 2009; Fabry et
59 al., 2008; Iglesias-Rodriguez et al., 2008; Munday et al., 2010; Munday et al., 2009).

60

61 Aragonite is a metastable form of calcium carbonate that is produced by major
62 calcifiers in coral reef ecosystems, including reef building corals, and is the
63 predominant biogenic carbonate mineral in warm and shallow waters of the tropics
64 (Stanley and Hardie, 1998). The aragonite saturation state of seawater has been used
65 as a proxy for estimating net calcification rates for corals e.g. Langdon (2005).

66 Projections suggest that by as early as 2050 growth rates of reef building coral may

67 slow to levels such that coral reefs may start to dissolve (Silverman et al., 2009). The
68 impact of acidification combined with other stressors, such as ocean warming, has
69 implications for the health, longer-term sustainability and biodiversity of reef
70 ecosystems (Doney et al., 2012; Dore et al., 2009).

71

72 The impact of these changes on the marine environment is of fundamental importance
73 for the management of future marine resources, for nations like Australia with its
74 extensive coastline and regions of international significance such as the Great Barrier
75 Reef. A historical record of the changes that have occurred since the preindustrial
76 period allows us to (i) correctly attribute observed responses over the historical
77 period; (ii) assess how well climate models represent spatial patterns of ocean
78 acidification for the period that overlaps observations (e.g. IPCC AR5); (iii) quantify
79 the magnitude of seasonal variability, and identify the drivers of this variability; and
80 (iv) provide important boundary conditions for high resolution regional models.

81

82 Despite the potential impacts of ocean acidification for the Australian region, the
83 number of carbonate chemistry measurements remains sparse. The few datasets
84 collected only characterise variability and the mean state in specific environments e.g.
85 (Shaw et al., 2012; Albright et al., 2013) or attempt to synthesize these into regional
86 or habitat-based studies e.g. Gagliano et al. (2010). The only seasonally-resolved
87 observational dataset available to characterize the mean state around Australia in the
88 present day is Takahashi et al. (2014), but this data has coarse resolution and only
89 focuses on the open ocean areas. Studies that have reconstructed the longer-term
90 variability of ocean acidification from coral proxies have been of regional scale, and
91 are temporally coarse e.g. Pelejero et al. (2005) and Calvo et al. (2007).

92

93 The goals of our study are: (i) reconstruct the observed variability and mean state in
94 pH and aragonite saturation state in the present day around Australia at high spatial
95 resolution and (ii) reconstruct the changes that have occurred in the Australian region
96 over the last 140 years (1870-2013). To this end, we first develop a new salinity-
97 alkalinity relationship for Australian waters based on observations collected around
98 Australia over the last two decades. We then assess our reconstructed pH and
99 aragonite saturation state fields with data collected around Australia at the Integrated

100 Marine Observing System National Reference Stations (IMOS-NRS; Lynch et al.,
101 2014). Finally, we present the reconstructed aragonite saturation state and pH in the
102 Australian region and discuss the seasonal and long-term changes in these fields. The
103 reconstructed fields as well as the calcite saturation state, dissolved inorganic carbon
104 dioxide (DIC), total alkalinity (TALK), sea surface temperature and salinity are all
105 available online at <http://imos.aodn.org.au>.

106
107

108 **3. Methods**

109 In this study we focus on the Australian region (Figure 1) delineated nominally by the
110 Subtropical Front (45° S) in the south and the equator (0°) in the north, and between
111 95°E and 170° E. This region encompasses part of the eastern Indian Ocean and
112 Indonesian Seas and a large part of the Tasman and Coral Seas. The seasonal cycle of
113 physical, chemical, and biological properties of the surface ocean mixed layer in this
114 region are described in Condie and Dunn (2006), and will not be described further in
115 this paper. The characterization of the carbon system requires two of six potential
116 carbon parameters (i.e. pH, total dissolved inorganic carbon, total alkalinity, partial
117 pressure of carbon dioxide $p\text{CO}_2$, bicarbonate, carbonate), from which all the
118 parameters of the ocean carbon system can be calculated. We first use $p\text{CO}_2$ and total
119 alkalinity to reconstruct the changes in ocean acidification.

120

121 Oceanic values of $p\text{CO}_2$ were taken from an updated version of Sasse et al. (2013)
122 that used a self-organizing multiple linear output (SOMLO) approach to predict $p\text{CO}_2$
123 values around Australia on a 1° x 1° degree grid each month for the nominal year of
124 2000. The SOMLO approach utilizes a global network of bottle-derived $p\text{CO}_2$ and
125 corresponding standard hydrographic parameters (SHP; temperature, salinity,
126 dissolved oxygen and phosphate; N=17753), collected from more than 263 cruises
127 and the HOTS and BATS time series sites, for more information on the individual
128 cruise data please see Table A1 in Sasse et al (2013). This data was first clustered into
129 49 neurons (or bins) based on similarities and homogeneity. Principle component
130 regressions were then derived between $p\text{CO}_2$ and the SHP using data within each
131 neuron. This can be thought of as a local-scale optimization, which follows the
132 nonlinear clustering routine. To then predict $p\text{CO}_2$ values for any set of SHP, a

133 similarity measure is first used to establish which neuron best represents the SHP
134 measurements, once established, pCO₂ values are predicted using the regression
135 parameters of that neuron. Independent testing by Sasse et al. (2013) reveals the
136 SOMLO approach predicts open-ocean pCO₂ values with a global uncertainty of 22.5
137 μatm (RMSE), which decreases to 16.3 μatm (RMSE; N=859) within the Australia
138 region. Monthly pCO₂ climatologies presented in Sasse et al. (2013) were derived
139 using the World Ocean Atlas (WOA) 2009 product (Antonov et al., 2010; Garcia et
140 al., 2010a; Garcia et al., 2010b; Locarnini et al., 2010), which we update here via the
141 WOA 2013 product (Garcia et al., 2014a, b; Locarnini et al., 2013; Zweng et al.,
142 2013). We note that these pCO₂ values provide significantly higher spatial data
143 coverage than the global climatology of Takahashi et al. (2009).

144

145 To extend the oceanic pCO₂ values into the past and the future, the value of ΔpCO₂
146 (pCO_{2air} - pCO_{2sea}) was first calculated using the oceanic pCO₂ values of Sasse et al.
147 (2013) for the year 2000. This ΔpCO₂ value was then transformed into a time series
148 of oceanic pCO₂ between 1870 to 2013, by adding this to the observed atmospheric
149 CO₂ value over this period using the atmospheric history constructed by Le Quéré et
150 al (2015).

151 As only limited measurements of total alkalinity (TALK) exist in the Australian
152 region, we develop and use the relationship between TALK and salinity to estimate
153 TALK in the Australian region. While many studies have quantified this relationship
154 globally e.g. Takahashi et al. (2014) and Lee et al. (2006) and regionally e.g.
155 Kuchinke et al. (2014), to date no specific relationship has been developed for the
156 entire Australian region.

157 To develop this relationship 2772 concomitant measurements of salinity and alkalinity
158 collected in the Australian region over the last two decades were used. (Table 1;
159 Figure 1). From this data we determined our alkalinity-salinity relationship to be:

160

$$161 \quad \text{TALK } (\mu\text{mol/kg}) = (2270.0 \pm 0.1) + (64.0 \pm 0.3) * (\text{SAL} - 35.) \quad (1)$$

162

163 This relationship is based on a type 2 linear regression, accounting for uncertainty in
164 both the salinity and TALK measurements of 0.05 and 3 μmol/kg respectively. This

165 new relationship was applied to the climatology of salinity ($0.5^\circ \times 0.5^\circ/\text{daily}$) taken
166 from the CSIRO Atlas of Regional Seas 2012 (CARS; Ridgway et al., 2002) as, at
167 present, no long-term high spatial and temporal resolution observations of ocean
168 surface salinity exist around Australia (nor globally). Nevertheless, based on sparse
169 measurements Durack and Wijffels (2010) suggested that there has been an
170 amplification of the global hydrological cycle that has resulted in surface salinity
171 changes over the last 50 years. Their estimated changes around Australia are not
172 uniform and are typically less than ± 0.1 , which introduces only a $6.4 \mu\text{mol/kg}$ change
173 in TALK for the 50-year period. The influence of the changes on the carbonate
174 chemistry (pH and aragonite saturation state changes of about 0.001 and 0.02
175 respectively), are small compared to the changes predicted from increasing
176 atmospheric CO_2 thereby allowing us to assume that the CARS salinity used has not
177 changed in our calculations.

178

179 Sea surface temperature (SST) measurements from 1870 to the present day were
180 obtained from the HadISST v1.1 dataset ($1^\circ \times 1^\circ$; Rayner et al., 2003). Higher
181 resolution datasets do exist, e.g. NOAA OI V2 ($0.25^\circ \times 0.25^\circ$; Reynolds et al., 2007),
182 but none have estimates beyond the last 3 decades, and we chose the $1^\circ \times 1^\circ$ product to
183 extend our reconstruction back to the pre-industrial period.

184 We first calculated DIC from TALK, SST and pCO_2 in the period 1870-2013, using
185 the method following Lenton et al. (2012) that used the dissociation constants of
186 Mehrbach et al. (1973) refitted by Dickson and Millero (1987). Our implementation
187 of carbonate chemistry is derived from the OCMIP3 framework (O. Aumont, C. Le
188 Quéré, and J. C. Orr, NOCES Project Interannual HOWTO, 2004, available at
189 <http://www.ipsl.jussieu.fr/OCMIP/>).

190

191 This approach calculates the magnitude of the seasonal cycle of DIC, rather than
192 pCO_2 . The pCO_2 seasonality changes over time in response to changes in the Revelle
193 factor and will influence the air-sea gradient in pCO_2 , which drives net flux across the
194 air-sea boundary e.g. Hauck and Völker (2015). To correct for this, we first calculated
195 the (detrended) seasonal anomaly of DIC in the period 1995-2006. We then added this
196 seasonal cycle of DIC to the (deseasonalised) long-term DIC record (1870-2013).

197 This allows us to reconstruct the historical DIC fields, and the changes in the

198 magnitude of the oceanic pCO₂ in response to the Revelle Factor to be accounted for.

199 We then added this seasonal cycle to the deseasonalised long-term DIC record (1870-
200 2013) to reconstruct the DIC fields, thereby allowing pCO₂ to change. The
201 reconstructed DIC fields were then used in conjunction with our derived TALK fields
202 to calculate changes in ocean acidification in the period 1870-2013. As the resolution
203 of SST and pCO₂ fields are nominally 1°x1° monthly fields, all values were calculated
204 on a 1°x1° grid at in-situ temperatures. The values of pH were calculated using the
205 total scale following recommendations of Riebesell et al. (2010) while aragonite and
206 calcite saturation states were calculated following Mucci (1983). To assess the
207 uncertainty in the reconstructed ocean acidification values, we compared these with
208 the values calculated from individual cruises, this allowed us to estimate the
209 uncertainty (RSME) to be 0.02 and 0.1 in pH and aragonite saturation state
210 respectively.

211 **4. Results and Discussion**

212 **4.1 Assessment of the mean state and seasonal variability at coastal NRS sites**

213 The ability of our reconstruction to predict the mean state and seasonality of ocean
214 acidification around Australia was evaluated by comparing our calculated aragonite
215 saturation state and SST data with carbonate chemistry and SST measurements made
216 over the last few years from seven of the eight Australian IMOS-NRS sites (Figure 2;
217 <https://imos.aodn.org.au>). The Darwin NRS site was not used in the comparison due
218 to the small number of measurements at this site. To assess how well the observed
219 response at the NRS sites were captured, we calculated both the correlation
220 coefficient (*R*) and the bias (or bias function) shown in Table 2.

221 The observed responses from the NRS sites compared with HadiSST are shown in
222 Figure 3. There is a good correlation in SST at all sites ($r > 0.84$, Table 2) providing
223 confidence that HadiSST represents the character of the seasonal variability. However
224 while HadiSST captures the SST variability, there were some biases in the mean SST
225 value (Table 2). These biases, e.g. Rottneest Island, likely reflect local process in the
226 coastal environment at the NRS e.g. Lima and Wethey (2012) that are poorly captured
227 by the much larger spatial scale of the HadiSST product.

228 The reconstructed aragonite saturation state (Ω_{AR}) shows good agreement with values
229 calculated from observations (Figure 4). The implication is that the salinity - total
230 alkalinity relationship and calculated pCO_2 fields, which are derived mostly from
231 offshore data, are valid for most of the IMOS-NRS sites, which tend to be located on
232 the outer shelf. Exceptions are the Ningaloo and Yongala sites, where our
233 reconstruction overestimates the observed values of aragonite saturation state while
234 SST agrees well with HadiSST (Table 2). The total alkalinity - salinity relationship
235 may not hold at these two sites due to the influence of net calcification on nearby
236 coral reef systems and possibly sediment-water exchange that could alter the total
237 alkalinity e.g. Shaw et al. (2012).

238 Apart from the offsets at the Yongala and Ningaloo sites, the reconstructed aragonite
239 saturation state does recreate the range determined at most locations (e.g. Maria
240 Island, Port Hacking, Rottneest, and North Stradbroke Island). Limited sampling at
241 Kangaroo Island, Esperance and Ningaloo sites prevented direct comparisons of the
242 seasonal variability, although the reconstructed variability appears plausible based on
243 available measurements.

244 Overall the ability of our reconstruction to capture the mean state and variability of
245 ocean acidification at the IMOS-NRS sites, gives us confidence in the reconstruction
246 of ocean acidification in the shelf and offshore waters around Australia, and to extend
247 our reconstruction back in time.

248

249 **4.2 Annual mean state**

250 The mean state of aragonite saturation state around Australia for the period 2000-2009
251 is shown in Figure 5. The mean state shows a strong latitudinal gradient in aragonite
252 saturation increasing from values of 1.8 in the southern part of the domain to values
253 greater than 3.9 across Northern Australia and into the Coral Sea. The Coral Sea and
254 Western Pacific form part of the coral triangle, a globally significant region in terms
255 of coral and marine diversity (Bell et al., 2011). We see that our reconstructed values
256 in the Coral Sea and into the Western Pacific are also consistent with the
257 observational values of 3.9 calculated by Kuchinke et al. (2014) in this region. This
258 value is well above 3.5, considered to be a key threshold at which corals move from

259 healthy to marginal conditions (Guinotte et al., 2003).

260 Ricke et al. (2013), using results from an ensemble of CMIP5 simulations and
261 GLODAP data reported that in the Coral Sea, the present-day values of aragonite
262 saturation state are much less than the 3.5 threshold (Guinotte et al., 2003). These
263 differences are explained by their correction of the CMIP5 simulations to GLODAP
264 DIC and TALK values (Key et al., 2004) that have very few measurements in this
265 region.

266 The annual mean state of pH for the period 2000-2009 is shown in Figure 5. In
267 contrast with aragonite saturation state there is an increasing latitudinal gradient from
268 ~8.1 in Northern Australia to ~8.14 in Southern Australia. The reconstructed values
269 show good agreement with observations collected on the southern Papua New Guinea
270 coast by Fabricius et al. (2011). However, south of Australia, the pH decreases again
271 to values comparable with those seen in Northern Australia.

272 The spatial gradients of pH and aragonite saturation state as function of latitude are
273 consistent with the large-scale gradients calculated from observations of carbonate
274 chemistry from GLODAP (Key et al., 2004). The distribution of aragonite saturation
275 state is set by both the large-scale distribution of SST, which shows a strong
276 latitudinal gradient, and TALK. Consequently the spatial differences between
277 aragonite saturation state and pH are driven by temperature e.g. Zeebe and Wolf-
278 Galdrow (2001).

279

280 **4.3 The Seasonal Cycle**

281 The seasonal standard deviation (2-sigma) of aragonite saturation state and pH reveal
282 large spatial differences in the magnitude of the seasonal variability (Figure 5, lower
283 panels). Large seasonality in aragonite saturation state is evident at > 0.4 units. This
284 spatial pattern of seasonality is quite heterogeneous, with the largest variability
285 occurring along the East Coast of Australia, in the Tasman Sea, and off Southern
286 Australia. The low seasonal variability predicted in the Coral Sea means that
287 aragonite saturation state is above 3.5 even in the winter months. Strong and
288 heterogeneous seasonality in pH is also present at > 0.06 units, around Australia, with

289 the largest range in Southern Australia.

290 The locations of large seasonality in aragonite saturation state and pH off Southern
291 Australia are associated with regions of deep winter mixing > 200m (Condie and
292 Dunn, 2006). Here, the seasonal deepening of the mixed layer in winter supplies
293 carbon, alkalinity and nutrients to the surface ocean, which in turn alter the chemistry
294 of the surface waters inducing large seasonal variability in ocean acidification values
295 in the surface ocean. That the large seasonal variability in aragonite saturation state is
296 not associated with large seasonal variability in pH along the East Coast of Australia
297 and in the Tasman Sea, suggests that here the dominant driver of seasonality
298 variability is SST rather than ocean dynamics.

299 An important consequence of the decoupling of the spatial patterns of pH and
300 aragonite saturation state is that the biological responses to ocean acidification at the
301 seasonal scale may also be decoupled as the susceptibility to pH and aragonite
302 saturation varies between organisms. This has implications for understanding
303 ecosystem responses to ocean acidification.

304 Areas of large seasonal variability are also present along parts off northern Australia
305 and off Papua New Guinea. These are primarily driven by large seasonal changes in
306 sea surface salinity driving changes in TALK and DIC which influences the pH and
307 aragonite saturation state.

308

309 **4.4 Comparison with Takahashi et al (2014)**

310 In this section the reconstructed annual mean and seasonality of pH and aragonite
311 saturation state are compared with those that calculated nominally for 2005
312 (Takahashi et al., 2014); hereafter-denoted T14 (Figure 6). The data of T14 are based
313 on oceanic pCO₂ measurements and regional potential alkalinity versus salinity
314 relationships, at a resolution of 4°x5°. Since T14 excludes Equatorial Pacific (north of
315 8°S) data and coastal data, we can only compare our results T14 away from these
316 regions.

317 The T14 spatial pattern of annual mean aragonite saturation state appears to be in

318 reasonable agreement with our reconstruction for most waters around Australia. An
319 exception is off Northwestern Australia where the mean aragonite saturation state of
320 T14 appears to be an under-estimate. Large differences in the seasonal changes also
321 occur off the east coast of Australia and to the South of Australia. The magnitude of
322 the seasonal variability (in T14) is lower than our reconstruction.

323 The pH values of T14 and our reconstruction both show the highest values in the
324 subtropical waters, although T14 mean values are higher off eastern Australia and
325 lower to the South of Australia. Overall there is quite poor agreement in both the
326 magnitude and spatial pattern of pH variability for most regions.

327 That the spatial pattern of the seasonal cycle of aragonite saturation state is not
328 reproduced along the East Coast of Australia and in the Tasman Sea, and the
329 variability in Southern Australia is not seen in either pH nor aragonite saturation state,
330 suggests that while the seasonal response of SST is captured in T14, the seasonal
331 ocean dynamics are not well represented. Furthermore the magnitude of the seasonal
332 cycle appeared to be underestimated in T14, this likely reflects the coarser resolution
333 of T14 product than our reconstruction ($4^{\circ}\times 5^{\circ}$ vs. $1^{\circ}\times 1^{\circ}$) and the spatial interpolation
334 required to generate T14.

335 As a result of this analysis we believe that in the Australian region our reconstruction
336 offers an improved and higher resolution representation of the mean state and
337 seasonality than T14. This comparison also underscores the need for such ongoing
338 regional analyses, and the limitations of using large-scale global products such as T14
339 to understand regional variability and change.

340

341 **4.5 Historical Changes**

342 The historical change in ocean acidification since 1870 is represented in Figure 7 by
343 the changes in the mean annual values of pH and aragonite saturation state between
344 the period 1870-1889 and 1990-2009. The corresponding changes in sea surface
345 temperature (HadiSST; Rayner et al., 2003) are shown over the same period in Figure
346 8, indicate a small net warming of the waters around Australia. This warming has
347 been relatively uniform with the exception of the northern edge of the Southern

348 Ocean, and Southeastern Australia which has been identified as a marine hotspot
349 Hobday and Pecl (2013). Consequently the SST changes alone cannot explain the
350 large ocean acidification changes, suggesting these are due to changes in ocean
351 carbon uptake, rather than changes in SST. The changes with time in pH and
352 saturation state at the IMOS-NRS sites are plotted in Figure 9.

353 We estimate that over the last 120 years there has been a (spatial) mean decrease in
354 aragonite saturation state of 0.49. However as illustrated in Figure 9, these decreases
355 are not constant with time and the change in aragonite saturation state is accelerating.
356 There is also a strong latitudinal gradient in magnitude of the decrease, with larger
357 changes occurring in Northern Australian waters (Ningaloo and North Stradbroke
358 Island) and smaller changes to the south (Maria Island). This pattern of change around
359 Australia is consistent with large-scale chemical buffering capacity of the ocean
360 (Revelle factor) which increases from ~ 9 at the equator to >11 at bottom of the study
361 region e.g. Sabine et al. (2004).

362 Consistent with aragonite saturation state over the last 120 years there has been a net
363 decrease in pH of 0.09 units, very close to the estimated global decrease of 0.1 pH by
364 Caldeira and Wickett (2003) over a similar period. Consistent with aragonite
365 saturation a strong latitudinal gradient in pH is evident, but it is the inverse. The
366 largest changes in pH have occurred in Southern Australia e.g. Maria Island (Figure
367 9), with the smallest changes in Northern Australian waters (e.g. Yongala (Figure 9) is
368 about 75% of the change experienced in the south). This spatial response of pH is
369 primarily set by the gradient of ocean mean temperature that acts to increase pH in
370 colder waters (Figure 8).

371

372 **4.7 Robustness of the reconstruction**

373 The reconstructed time series of aragonite saturation state and pH are driven wholly
374 by SST and atmospheric CO₂, thereby neglecting any changes in salinity and/or
375 biological production. Observationally, studies have suggested that in some regions
376 around Australia changes in salinity over the last 50 years have occurred e.g. Durack
377 and Wijffels (2010), while other regions have remained constant over the last 200
378 years e.g. Calvo et al. (2007). If we assume, consistent with Durack et al. (2012), that

379 the changes are related to evaporation – precipitation (E-P) rather than local riverine
380 input which can have large local inputs of DIC, TALK and potentially nutrients
381 (Hieronymus and Walin, 2013), then any increase in salinity can be treated as
382 freshwater input only. Consequently given the small trends, relative to the mean, and
383 the very low sensitivity of oceanic $p\text{CO}_2$ to freshwater input ($< 1\%$), it is highly
384 unlikely that such changes would make such a significant difference on pH or
385 aragonite over the last 50 years. This is perhaps not surprising given that changes in
386 freshwater water input act as a dilution flux i.e. acting equally on DIC and total
387 alkalinity (Lenton et al., 2012).

388

389 The roles of nutrients driving variability and change in ocean acidification are also not
390 considered in this study, as we assume that nutrients are zero around Australia. While
391 this is not strictly true, most waters around Australia are oligotrophic in nature
392 (Condie and Dunn, 2006). If the climatological values of silicate and nitrate from
393 CARS (Ridgway et al., 2002) are used to calculate carbonate chemistry, we find only
394 a small bias (0.0007 in aragonite saturation state and 0.005 in pH) in our
395 reconstruction (well within the uncertainty). While we would like to have used a time-
396 evolving field, analogous to salinity, at present no long-term time series are available
397 to use in this reconstruction.

398 In this study we assumed that the seasonal air-sea disequilibrium ($\Delta p\text{CO}_2$) is
399 seasonally time invariant i.e. no interannual variability. While some studies have
400 argued this variability maybe important at shorter-term timescales e.g. Sitch et al
401 (2015), it is less clear how important these are on longer time series e.g. McKinley et
402 al (2011). This is further complicated as the existing products of oceanic $p\text{CO}_2$ fields
403 e.g. Landschützer et al. (2014) only extend back in time several decades reflecting the
404 limit of historical observations. Nevertheless to assess how important this term could
405 be, we assumed an upper bound from the published study of McNeil and Matear
406 (2008) who, in the more dynamically and biologically active Southern Ocean,
407 calculated the error introduced by assuming a fixed (air-sea) disequilibrium term.
408 From this study we can see that for an equivalent increase in (future) atmospheric CO_2
409 levels, the error introduced into our calculation of pH and aragonite saturation state
410 falls well within the reported uncertainty of our reconstruction.

411 **5. Conclusion**

412 To explore how Australia's marine environment has changed, we have synthesized
413 newly acquired in-situ observations of carbon chemistry around Australia to: (i)
414 provide an new estimate of the mean state and seasonality of pH and aragonite
415 saturation state; and (ii) reconstruct the changes in ocean acidification around
416 Australia since 1870.

417 In this work we developed a new total alkalinity-salinity relationship for the
418 Australian region. This relationship was used in conjunction with observed salinity
419 and oceanic and atmospheric CO₂ and SST data, to reconstruct the present and past
420 changes in pH and aragonite saturation state. Our reconstructed fields were compared
421 against the Takahashi et al (2014) climatology, and high-resolution data collected at
422 the IMOS-NRS sites. We found good agreement between our reconstructed fields for
423 the observed annual mean and seasonal cycles at the shelf IMOS-NRS sites except
424 regions such as the Great Barrier Reef where near shore processes and coral reef
425 metabolism could alter the pH and saturation state.

426 Our regional reconstruction provides much higher spatial and temporal resolution than
427 previous global estimates. This highlights the importance of regional analyses and
428 reconstructions in estimating and understanding region changes. An important result
429 of this study is that at present the Coral Sea is not experiencing marginal conditions
430 (values of aragonite saturation state < 3.5) with respect to ocean acidification as has
431 been suggested.

432 Large changes in aragonite saturation state and pH have occurred over the last 140
433 years in response to increasing oceanic uptake of atmospheric CO₂. A net (spatial)
434 mean decrease in pH of 0.09 is seen in the period (1990-2009) – (1889-1870),
435 together with a net decrease in aragonite saturation state of 0.49, both of which are
436 consistent with previous estimates of the historical changes. Importantly, due to ocean
437 chemistry, the spatial pattern of the change in aragonite saturation state and pH are
438 different. In this study we found the largest changes in aragonite saturation state
439 occurred at mid and low latitudes, and the largest changes in pH occurred at higher
440 latitudes.

441 The large seasonal variability around Australia is heterogeneous, with distinctly

442 different spatial patterns in aragonite saturation state and pH, with the exception of
443 from South of Australia where variability is driven by deep winter mixing. For
444 aragonite saturation state, large seasonal variability occurs off the East Coast of
445 Australia and in Tasman Sea driven by seasonal variability in ocean temperatures
446 That the variability in aragonite saturation state and pH are spatially different over
447 temporal and regional scales, implies that biological responses and impacts are likely
448 vary. Further, this suggests that both pH and aragonite (or calcite) saturation state
449 need to be considered independently in assessing ecosystem responses and changes.
450 This historical reconstruction also provides useful information to link with biological
451 observations to help understand observed changes and aid in the design of future
452 work, thereby elucidating the consequences of Ocean Acidification. To facilitate this
453 all of the reconstructed data is available at <http://imos.aodn.org.au>

454 **6. Acknowledgments**

455 AL, BT and RJM acknowledge support from the Australian Climate Change Science
456 Program. TPS would like to acknowledge funding support for the CSIRO carbon
457 cluster. YN was supported by JSPS KAKENHI Grant Number 26220102. The authors
458 would like to thank the Integrated Marine Observing System (IMOS) for providing
459 data from the Australian National Research Sites (NRSs), and Kate Berry and Kristina
460 Patterson for their analysis of the observed carbon data.

461 **7. References**

- 462 Albright, R., Langdon, C., and Anthony, K. R. N.: Dynamics of seawater carbonate
463 chemistry, production, and calcification of a coral reef flat, Central Great Barrier Reef,
464 *Biogeosciences*, 10, 6747-6758, 2013.
- 465 Antonov, J. I., Seidov, D., Boyer, T. P., Locarnini, R. A., Mishonov, A. V., Garcia, H. E.,
466 Baranova, O. K., Zweng, M. M., and Johnson, D. R., *World Ocean Atlas 2009, Volume 2:*
467 *Salinity*, in, edited by: Levitus, S., NOAA Atlas NESDIS 69, U.S. Government Printing
468 Office, Washington, D.C., 184 pp, 2010
- 469 Bell, J. D., JE, J., and AJ, H.: Vulnerability of Tropical Pacific Fisheries and Aquaculture to
470 Climate Change, Secretariat of the Pacific Community, Noumea, New Caledonia, 2011.
- 471 Caldeira, K., and Wickett, M. E.: Anthropogenic carbon and ocean pH, *Nature*, 425, 365-365,
472 Doi 10.1038/425365a, 2003.
- 473 Calvo, E., Marshall, J. F., Pelejero, C., McCulloch, M. T., Gagan, M. K., and Lough, J. M.:
474 Interdecadal climate variability in the Coral Sea since 1708 AD, *Palaeogeogr Palaeocl*, 248,
475 190-201, Doi 10.1016/J.Palaeo.2006.12.003, 2007.
- 476 Ciais, P., Sabine, C., Bala, G., Bopp, L., Brovkin, V., Canadell, J., Chhabra, A., Defriers, R.,
477 Galloway, J. N., Heinman, M., Jones, C. D., Le Quéré, C., Myneni, R. B., Piao, S., and
478 Thornton, P.: Carbon and Other Biogeochemical Cycles, in: *Climate Change 2013: The*
479 *Physical Science Basis. Contribution of Working Group I to the Fifth Assessment Report of*
480 *the Intergovernmental Panel on Climate Change* edited by: Stocker, T. F., Qin, D., Plattner,
481 G.-K., Tignor, M., Allen, S. K., Boschung, A., A, N., Xia, Y., V., B., and Midgley, P. M.,
482 Cambridge University Press, Cambridge, United Kingdom and New York 2013.
- 483 Condie, S. A., and Dunn, J. R.: Seasonal characteristics of the surface mixed layer in the
484 Australasian region: implications for primary production regimes and biogeography, *Marine*
485 *and Freshwater Research*, 57, 569-590, Doi 10.1071/Mf06009_Lr, 2006.
- 486 Dickson, A. G., and F. J. Millero, A comparison of the equilibrium constants for the
487 dissociation of carbonic acid in seawater media, *Deep Sea Res., Part I*, 34, 1733-1743,
488 doi:10.1016/0198-0149(87)90021-5, 1987
- 489 Doney, S. C., Balch, W. M., Fabry, V. J., and Feely, R. A.: Ocean Acidification: A Critical
490 Emerging Problem for the Ocean Sciences, *Oceanography*, 22, 16-+, Doi
491 10.5670/Oceanog.2009.93, 2009.
- 492 Doney, S. C., Ruckelshaus, M., Duffy, J. E., Barry, J. P., Chan, F., English, C. A., Galindo, H.
493 M., Grebmeier, J. M., Hollowed, A. B., Knowlton, N., Polovina, J., Rabalais, N. N.,
494 Sydeman, W. J., and Talley, L. D.: Climate Change Impacts on Marine Ecosystems, *Annu*
495 *Rev Mar Sci*, 4, 11-37, Doi 10.1146/Annurev-Marine-041911-111611, 2012.

496 Dore, J. E., Lukas, R., Sadler, D. W., Church, M. J., and Karl, D. M.: Physical and
497 biogeochemical modulation of ocean acidification in the central North Pacific, *P Natl Acad*
498 *Sci USA*, 106, 12235-12240, Doi 10.1073/Pnas.0906044106, 2009.

499 Durack, P. J., and Wijffels, S. E.: Fifty-Year Trends in Global Ocean Salinities and Their
500 Relationship to Broad-Scale Warming, *Journal of Climate*, 23, 4342-4362, Doi
501 10.1175/2010jcli3377.1, 2010.

502 Durack, P. J., Wijffels, S. E., and Matear, R. J.: Ocean Salinities Reveal Strong Global Water
503 Cycle Intensification During 1950 to 2000, *Science*, 336, 455-458, Doi
504 10.1126/Science.1212222, 2012.

505 Fabricius, K. E., Langdon, C., Uthicke, S., Humphrey, C., Noonan, S., De'ath, G., Okazaki,
506 R., Muehllehner, N., Glas, M. S., and Lough, J. M.: Losers and winners in coral reefs
507 acclimatized to elevated carbon dioxide concentrations, *Nat Clim Change*, 1, 165-169, Doi
508 10.1038/Nclimate1122, 2011.

509 Fabry, V. J., Seibel, B. A., Feely, R. A., and Orr, J. C.: Impacts of ocean acidification on
510 marine fauna and ecosystem processes, *Ices J Mar Sci*, 65, 414-432, Doi
511 10.1093/Icesjms/Fsn048, 2008.

512 Frolicher, T. L., and Joos, F.: Reversible and irreversible impacts of greenhouse gas emissions
513 in multi-century projections with the NCAR global coupled carbon cycle-climate model, *Clim*
514 *Dynam*, 35, 1439-1459, Doi 10.1007/S00382-009-0727-0, 2010.

515 Gagliano, M., McCormick, M. I., Moore, J. A., and Depczynski, M.: The basics of
516 acidification: baseline variability of pH on Australian coral reefs, *Marine Biology*, 157, 1849-
517 1856, Doi 10.1007/S00227-010-1456-Y, 2010.

518 Garcia, H. E., Locarnini, R. A., Boyer, T. P., Antonov, J. I., Baranova, O. K., Zweng, M. M.,
519 and Johnson, D. R. (2010a), *World Ocean Atlas 2009, Volume 3: Dissolved Oxygen*
520 *Apparent Oxygen Utilization, and Oxygen Saturation*, in, edited by: Levitus, S., NOAA Atlas
521 NESDIS 70, U.S. Government Printing Office, Washington, D.C., 344 pp.

522 Garcia, H. E., Locarnini, R. A., Boyer, T. P., Antonov, J. I., Zweng, M. M., Baranova, O. K.,
523 and Johnson, D. R., *World Ocean Atlas 2009, Volume 4: Nutrients (phosphate, nitrate,*
524 *silicate)*, in, edited by: Levitus, S., NOAA Atlas NESDIS 71, U.S. Government Printing
525 Office, Washington, D.C., 398 pp., 2010b

526 Garcia, H. E., Locarnini, R. A., Boyer, T. P., Antonov, J. I., Baranova, O. K., Zweng, M. M.,
527 Reagan, J. R., and Johnson, D. R., *World Ocean Atlas 2013, Volume 3: Dissolved Oxygen,*
528 *Apparent Oxygen Utilization, and Oxygen Saturation*, in, edited by: Levitus, S., and
529 Mishonov, A., NOAA Atlas NESDIS 75, 27 pp, 2014a

530

531 Garcia, H. E., Locarnini, R. A., Boyer, T. P., Antonov, J. I., Baranova, O. K., Zweng, M. M.,
532 Reagan, J. R., and Johnson, D. R., World Ocean Atlas 2013, Volume 4: Dissolved Inorganic
533 Nutrients (phosphate, nitrate, silicate), in, edited by: Levitus, S., and Mishonov, A., NOAA
534 Atlas NESDIS 76, 25, 25 pp., 2014b

535 Guinotte, J. M., Buddemeier, R. W., and Kleypas, J. A.: Future coral reef habitat marginality:
536 temporal and spatial effects of climate change in the Pacific basin, *Coral Reefs*, 22, 551-558,
537 Doi 10.1007/S00338-003-0331-4, 2003.

538 Hauck, J., and C. Völker, Rising atmospheric CO₂ leads to large impact of biology on
539 Southern Ocean CO₂ uptake via changes of the Revelle factor, *Geophys. Res. Lett.*, 42,
540 1459–1464, doi:10.1002/2015GL063070, 2015

541 Hieronymus, J., and Walin, G.: Unravelling the land source: an investigation of the processes
542 contributing to the oceanic input of DIC and alkalinity, *Tellus B*, 65, Artn 19683 Doi
543 10.3402/Tellusb.V65i0.19683, 2013.

544 Hobday, A. J., and Pecl, G. T.: Identification of global marine hotspots: sentinels for change
545 and vanguards for adaptation action, *Rev Fish Biol Fisheries*, 10.1007/s11160-013-9326-6,
546 2013.

547 Iglesias-Rodriguez, M. D., Halloran, P. R., Rickaby, R. E. M., Hall, I. R., Colmenero-
548 Hidalgo, E., Gittins, J. R., Green, D. R. H., Tyrrell, T., Gibbs, S. J., von Dassow, P., Rehm,
549 E., Armbrust, E. V., and Boessenkool, K. P.: Phytoplankton calcification in a high-CO₂
550 world, *Science*, 320, 336-340, Doi 10.1126/Science.1154122, 2008.

551 Key, R. M., Kozyr, A., Sabine, C. L., Lee, K., Wanninkhof, R., Bullister, J. L., Feely, R. A.,
552 Millero, F. J., Mordy, C., and Peng, T. H.: A global ocean carbon climatology: Results from
553 Global Data Analysis Project (GLODAP), *Global Biogeochemical Cycles*, 18, Artn Gb4031
554 Doi 10.1029/2004gb002247, 2004.

555 Kuchinke, M., Tilbrook, B., and Lenton, A.: Seasonal variability of aragonite saturation state
556 in the Western Pacific, *Mar Chem*, 161, 1-13, Doi 10.1016/J.Marchem.2014.01.001, 2014.

557 Langdon, C.: Effect of elevated pCO₂ on photosynthesis and calcification of corals and
558 interactions with seasonal change in temperature/irradiance and nutrient enrichment, *Journal*
559 *of Geophysical Research*, 110, 10.1029/2004jc002576, 2005.

560 Le Quéré, C., Moriarty, R., Andrew, R. M., Peters, G. P., Ciais, P., Friedlingstein, P., Jones,
561 S. D., Sitch, S., Tans, P., Arneeth, A., Boden, T. A., Bopp, L., Bozec, Y., Canadell, J. G.,
562 Chini, L. P., Chevallier, F., Cosca, C. E., Harris, I., Hoppema, M., Houghton, R. A., House, J.
563 I., Jain, A. K., Johannessen, T., Kato, E., Keeling, R. F., Kitidis, V., Klein Goldewijk, K.,
564 Koven, C., Landa, C. S., Landschützer, P., Lenton, A., Lima, I. D., Marland, G., Mathis, J. T.,
565 Metzl, N., Nojiri, Y., Olsen, A., Ono, T., Peng, S., Peters, W., Pfiel, B., Poulter, B., Raupach,
566 M. R., Regnier, P., Rödenbeck, C., Saito, S., Salisbury, J. E., Schuster, U., Schwinger, J.,

567 S  ferian, R., Segschneider, J., Steinhoff, T., Stocker, B. D., Sutton, A. J., Takahashi, T.,
568 Tilbrook, B., van der Werf, G. R., Viovy, N., Wang, Y. P., Wanninkhof, R., Wiltshire, A.,
569 and Zeng, N.: Global carbon budget 2014, 7, 47-85, doi:10.5194/essd-7-47-2015, 2015.

570 Lee, K., Tong, L. T., Millero, F. J., Sabine, C. L., Dickson, A. G., Goyet, C., Park, G. H.,
571 Wanninkhof, R., Feely, R. A., and Key, R. M.: Global relationships of total alkalinity with
572 salinity and temperature in surface waters of the world's oceans, *Geophys Res Lett*, 33, -, Artn
573 L19605 Doi 10.1029/2006gl027207, 2006.

574 Lenton, A., Metzl, N., Takahashi, T., Kuchinke, M., Matear, R. J., Roy, T., Sutherland, S. C.,
575 Sweeney, C., and Tilbrook, B.: The observed evolution of oceanic pCO₂ and its drivers over
576 the last two decades, *Global Biogeochemical Cycles*, 26, Artn Gb2021, Doi
577 10.1029/2011gb004095, 2012.

578 Lima, F. P., and Wethey, D. S.: Three decades of high-resolution coastal sea surface
579 temperatures reveal more than warming, *Nat Commun*, 3, Artn 704
580 Doi 10.1038/Ncomms1713, 2012.

581 Locarnini, R. A., Mishonov, A. V., Antonov, J. I., Boyer, T. P., Garcia, H. E., Baranova, O.
582 K., Zweng, M. M., and Johnson, D. R., *World Ocean Atlas 2009, Volume 1: Temperature*, in,
583 edited by: Levitus, S., Ed. NOAA Atlas NESDIS 68, U.S. Government Printing Office,
584 Washington, D.C., 184 pp., 2010

585 Locarnini, R. A., Mishonov, A. V., Antonov, J. I., Boyer, T. P., Garcia, H. E., Baranova, O.
586 K., Zweng, M. M., Paver, C. R., Reagan, J. R., Johnson, D. R., Hamilton, M., and Seidov, D.
587 *World Ocean Atlas 2013, Volume 1: Temperature*, in, edited by: S. Levitus, E., and A.
588 Mishonov, T. E., NOAA Atlas NESDIS 73, 40 pp, 2013

589 Lynch, T. P., Morello, E. B., Evans, K., Richardson, A., Rochester, J. W. C., Steinberg, C. R.,
590 Roughan, M., Thompson, P., Middleton, J. F., Feng, M., Sherrington, R., Brando, V.,
591 Tilbrook, B., Ridgway, K., Allen, S., Doherty, P., Hill, K., and Moltmann, T. C.: IMOS
592 National Reference Stations: a continental wide physical, chemical and biological coastal
593 observing system. , *PLOS One*, 9(12): e113652, doi:10.1371/journal.pone.0113652, 2014.

594 Matear, R. J., and Lenton, A.: Quantifying the impact of ocean acidification on our future
595 climate, *Biogeosciences*, 11, 3965-3983, doi: 10.5194/Bg-11-3965-2014, 2014.

596 McNeil, B. I. and R.J. Matear: Southern Ocean acidification: A tipping point at 450-ppm
597 atmospheric CO₂, *PNAS* 105 (48), 18860-18864, doi: 10.1073/pnas.0806318105, 2008

598 McKinley, G. A., Fay, A. R., Takahashi, T., and N.Metzl: Convergence of atmospheric and
599 North Atlantic carbon dioxide trends on multidecadal timescales, *Nature Geoscience*
600 **4**, 606–610 doi:10.1038/ngeo1193, 2011

601 Mehrbach, C., C. H. Culberson, J. E. Hawley, and R. M. Pytkowicz, Measurement of the
602 apparent dissociation constants of carbonic acid in seawater at atmospheric pressure, *Limnol.*

603 Oceanogr., 18, 897–907,doi:10.4319/lo.1973.18.6.0897, 1973.

604 Mucci, A.: The Solubility of Calcite and Aragonite in Seawater at Various Salinities,
605 Temperatures, and One Atmosphere Total Pressure, Am J Sci, 283, 780-799, 1983.

606 Munday, P. L., Donelson, J. M., Dixson, D. L., and Endo, G. G. K.: Effects of ocean
607 acidification on the early life history of a tropical marine fish, P Roy Soc B-Biol Sci, 276,
608 3275-3283, Doi 10.1098/Rspb.2009.0784, 2009.

609 Munday, P. L., Dixson, D. L., McCormick, M. I., Meekan, M., Ferrari, M. C. O., and Chivers,
610 D. P.: Replenishment of fish populations is threatened by ocean acidification, P Natl Acad Sci
611 USA, 107, 12930-12934, doi:10.1073/Pnas.1004519107, 2010.

612 Pelejero, C., Calvo, E., McCulloch, M. T., Marshall, J. F., Gagan, M. K., Lough, J. M., and
613 Opdyke, B. N.: Preindustrial to modern interdecadal variability in coral reef pH, Science, 309,
614 2204-2207, Doi 10.1126/Science.1113692, 2005.

615 Rayner, N. A., Parker, D. E., Horton, E. B., Folland, C. K., Alexander, L. V., Rowell, D. P.,
616 Kent, E. C., and Kaplan, A.: Global analyses of sea surface temperature, sea ice, and night
617 marine air temperature since the late nineteenth century, J Geophys Res-Atmos, 108, Artn
618 4407,doi:10.1029/2002jd002670, 2003.

619 Reynolds, R. W., Smith, T. M., Liu, C., Chelton, D. B., Casey, K. S., and Schlax, M. G.:
620 Daily high-resolution-blended analyses for sea surface temperature, Journal of Climate, 20,
621 5473-5496, Doi 10.1175/2007jcli1824.1, 2007.

622 Rieke, K. L., Orr, J. C., Schneider, K., and Caldeira, K.: Risks to coral reefs from ocean
623 carbonate chemistry changes in recent earth system model projections, Environ Res Lett, 8,
624 Artn 034003, Doi 10.1088/1748-9326/8/3/034003, 2013.

625 Ridgway, K. R., Dunn, J. R., and Wilkin, J. L.: Ocean interpolation by four-dimensional
626 weighted least squares - application to the waters around Australasia, Journal of Atmospheric
627 and Oceanic Technology, 19, 1357-1375, Doi 10.1175/1520-0426, 2002.

628 Riebesell, U., Fabry, V. J., Hansson, L., and Gattuso, J.-P.: Guide to best practices for ocean
629 acidification research and data reporting, Publications Office of the European Union.,
630 Luxembourg, 260, 2010.

631 Sabine, C. L., Feely, R. A., Gruber, N., Key, R. M., Lee, K., Bullister, J. L., Wanninkhof, R.,
632 Wong, C. S., Wallace, D. W. R., Tilbrook, B., Millero, F. J., Peng, T. H., Kozyr, A., Ono, T.,
633 and Rios, A. F.: The oceanic sink for anthropogenic CO₂, Science, 305, 367-371, Doi
634 10.1126/Science.1097403, 2004.

635 Sasse, T. P., McNeil, B. I., and Abramowitz, G.: A new constraint on global air-sea CO₂
636 fluxes using bottle carbon data, Geophys Res Lett, 40, 1594-1599, Doi 10.1002/Grl.50342,
637 2013.

638 Shaw, E. C., McNeil, B. I., and Tilbrook, B.: Impacts of ocean acidification in naturally
639 variable coral reef flat ecosystems, *J Geophys Res-Oceans*, 117, Artn C03038, Doi
640 10.1029/2011jc007655, 2012.

641 Silverman, J., Lazar, B., Cao, L., Caldeira, K., and Erez, J.: Coral reefs may start dissolving
642 when atmospheric CO₂ doubles, *Geophys Res Lett*, 36, Artn L05606
643 Doi 10.1029/2008gl036282, 2009.

644 Stanley, S. M., and Hardie, L. A.: Secular oscillations in the carbonate mineralogy of reef-
645 building and sediment-producing organisms driven by tectonically forced shifts in seawater
646 chemistry, *Palaeogeogr Palaeoclimatol*, 144, 3-19, Doi 10.1016/S0031-0182(98)00109-6, 1998.

647 Takahashi, T., Sutherland, S. C., Wanninkhof, R., Sweeney, C., Feely, R. A., Chipman, D.
648 W., Hales, B., Friederich, G., Chavez, F., Sabine, C., Watson, A., Bakker, D. C. E., Schuster,
649 U., Metzl, N., Yoshikawa-Inoue, H., Ishii, M., Midorikawa, T., Nojiri, Y., Kortzinger, A.,
650 Steinhoff, T., Hoppema, M., Olafsson, J., Arnarson, T. S., Tilbrook, B., Johannessen, T.,
651 Olsen, A., Bellerby, R., Wong, C. S., Delille, B., Bates, N. R., and de Baar, H. J. W.:
652 Climatological mean and decadal change in surface ocean pCO₂, and net sea-air CO₂ flux
653 over the global oceans, *Deep-Sea Res Pt II*, 56, 554-577, Doi 10.1016/J.Dsr2.2008.12.009,
654 2009.

655 Sitch, S., Friedlingstein, P., Gruber, N., Jones, S. D., Murray-Tortarolo, G., Ahlström, A.,
656 Doney, S. C., Graven, H., Heinze, C., Huntingford, C., Levis, S., Levy, P. E., Lomas, M.,
657 Poulter, B., Viovy, N., Zaehle, S., Zeng, N., Arneth, A., Bonan, G., Bopp, L., Canadell, J. G.,
658 Chevallier, F., Ciais, P., Ellis, R., Gloor, M., Peylin, P., Piao, S. L., Le Quéré, C., Smith, B.,
659 Zhu, Z., and Myneni, R.: Recent trends and drivers of regional sources and sinks of carbon
660 dioxide, *Biogeosciences*, 12, 653-679, doi:10.5194/bg-12-653-2015, 2015.

661 Takahashi, T., Sutherland, S. C., Chipman, D. W., Goddard, J. G., Ho, C., Newberger, T.,
662 Sweeney, C., and Munro, D. R.: Climatological distributions of pH, pCO₂, total CO₂,
663 alkalinity, and CaCO₃ saturation in the global surface ocean, and temporal changes at selected
664 locations, *Mar Chem*, 164, 95-125, doi: 10.1016/j.marchem.2014.06.004, 2014.

665 Zeebe, R. E. and Wolf-Gladrow. CO₂ in Seawater: Equilibrium, Kinetics, Isotopes. Elsevier
666 Oceanography Series, 65, pp. 346, Amsterdam, 2001

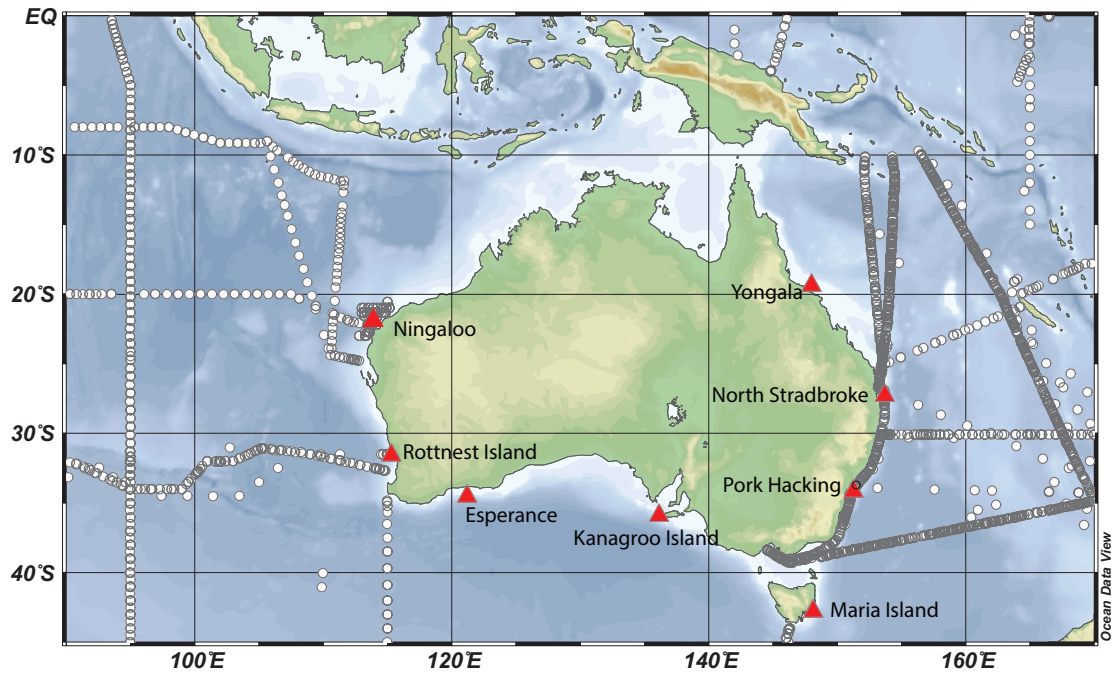
667 Zweng, M. M., Reagan, J. R., Antonov, J. I., Locarnini, R. A., Mishonov, A. V., Boyer, T. P.,
668 Garcia, H. E., Baranova, O. K., Johnson, D. R., D. Seidov, and Biddle, M. M. (2013), World
669 Ocean Atlas 2013, Volume 2: Salinity, in, edited by: Levitus, S., and Mishonov, A., NOAA
670 Atlas NESDIS 74, 39 pp.

671

672

673

674 **7. Figures and Tables**



675

676

677 Figure 1 Locations (circles) of the concomitant measurements of alkalinity and
678 salinity used to develop a new salinity-alkalinity relationship for the Australian
679 Region, the cruises are listed in Table 1. Overlain on this plot (red triangles) are the
680 locations of IMOS National Reference Stations (NRS) used in this study.

681

682

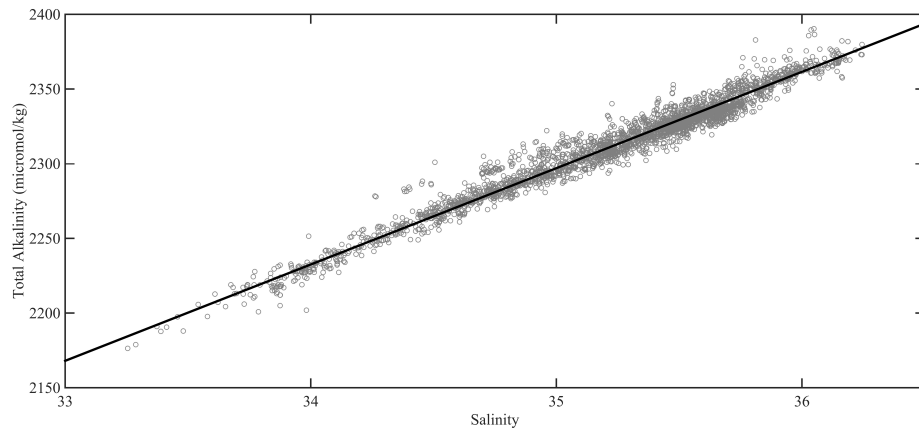
683

684

685

686

687



688

689

690 Figure 2 The new salinity-alkalinity relationship developed for the Australian Region

691 based on observations (Figure 1) collected in the period 1992-2011. The individual

692 cruises are listed in Table 1.

693

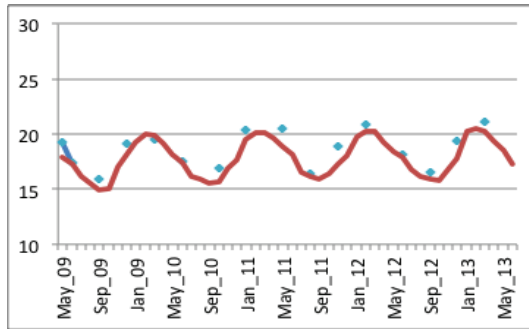
694

695

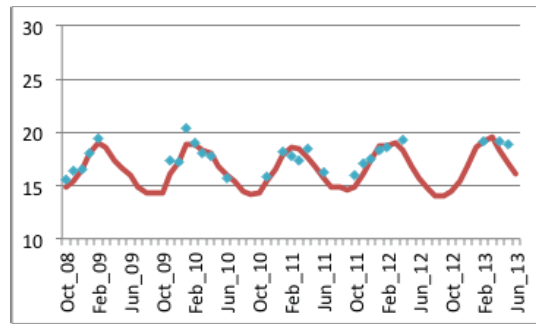
696

697

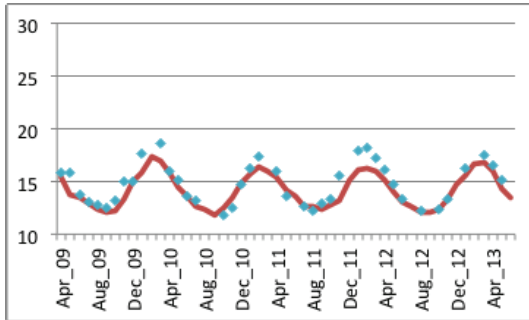
698



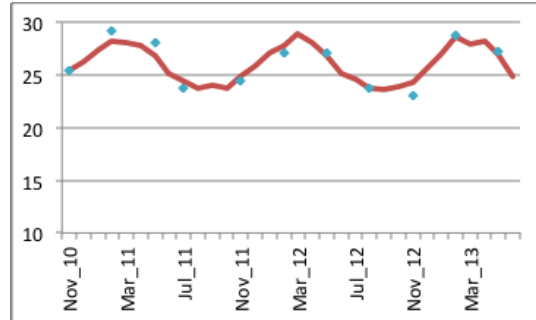
Esperance



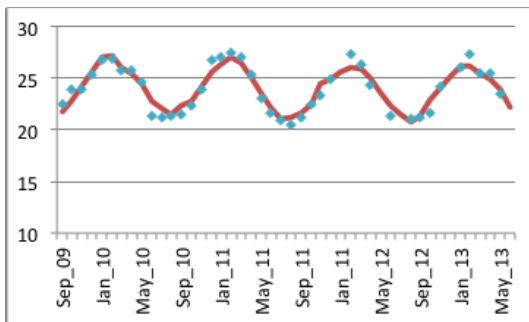
Kangaroo Island



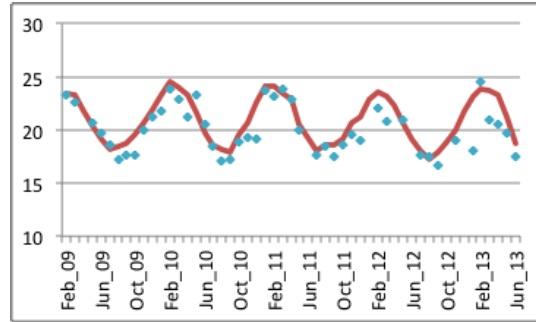
Maria Island



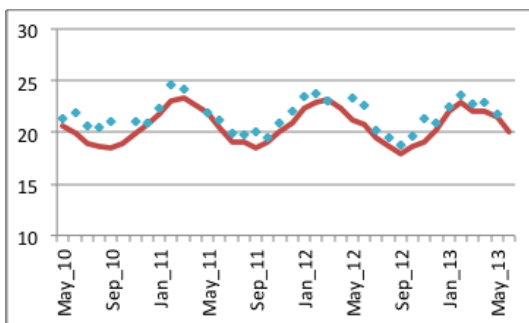
Ningaloo



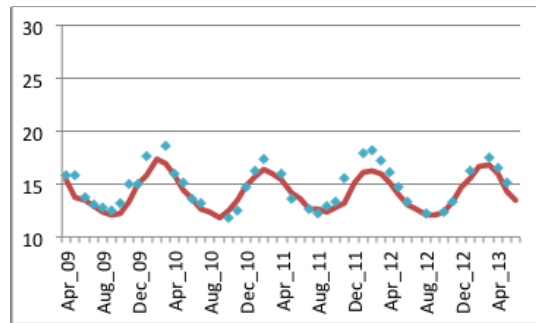
North Stradbroke



Port Hacking



Rottneest



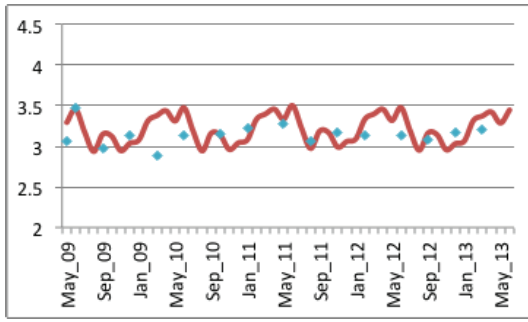
Yongala

699

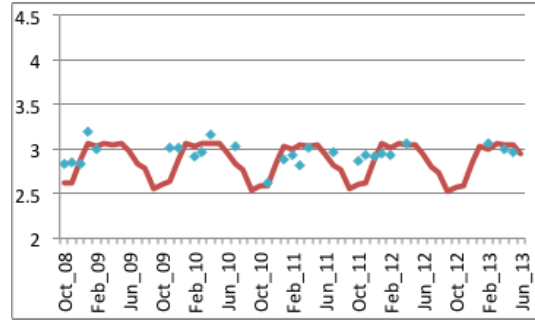
700

701

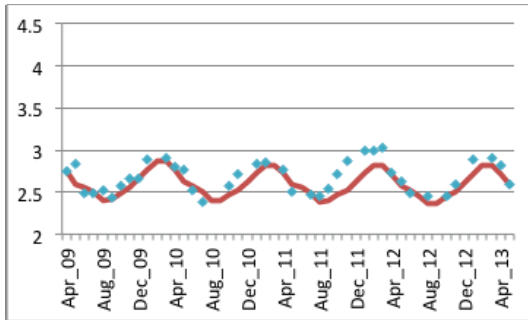
Figure 3 Comparison of sea surface temperature from the observations at the IMOS National Research Stations with HadiSST (Rayner et al, 2003)



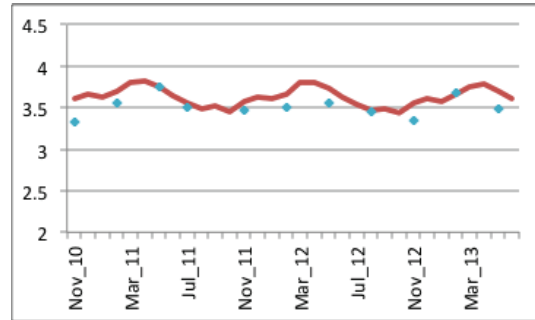
Esperance



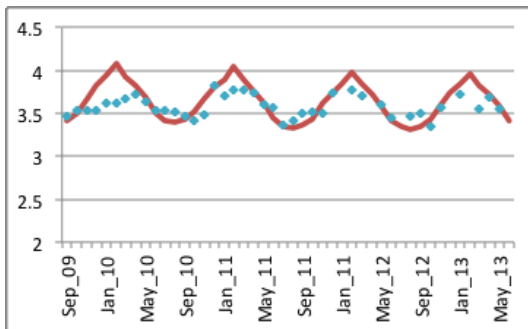
Kangaroo Island



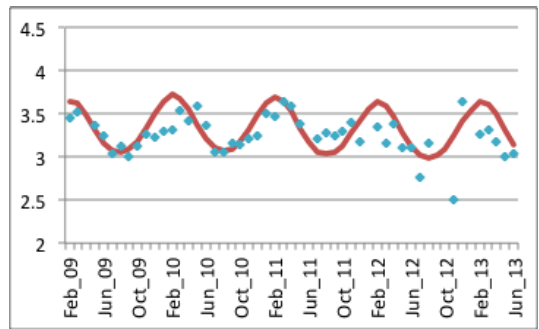
Maria Island



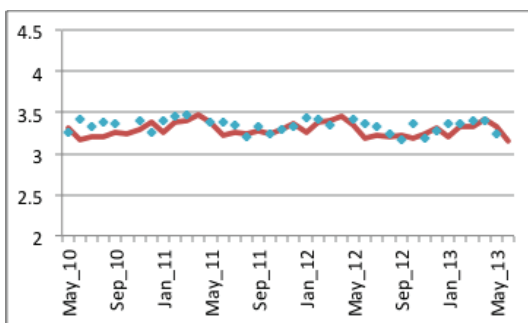
Ningaloo



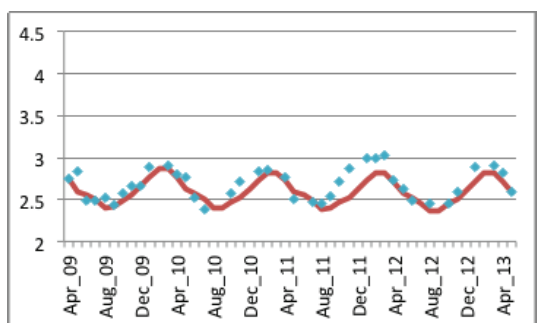
North Stradbroke



Port Hacking



Rottnest



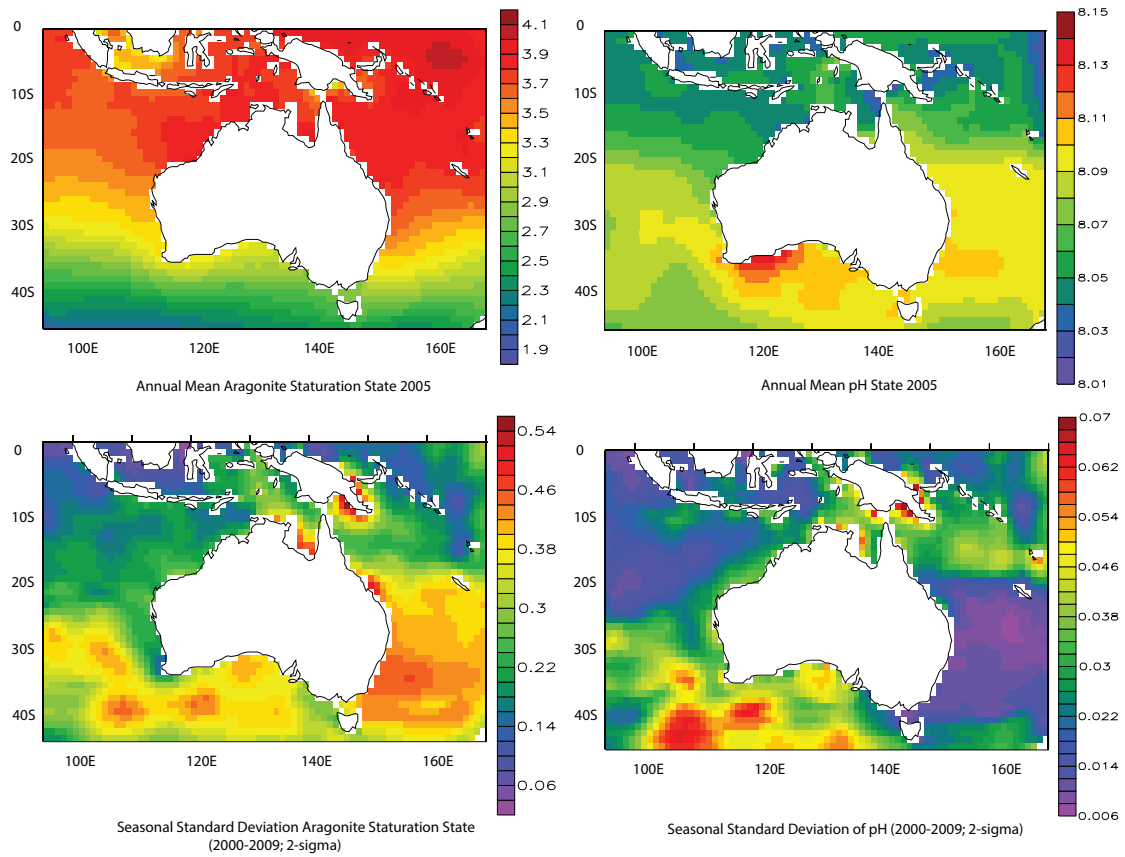
Yongala

702

703

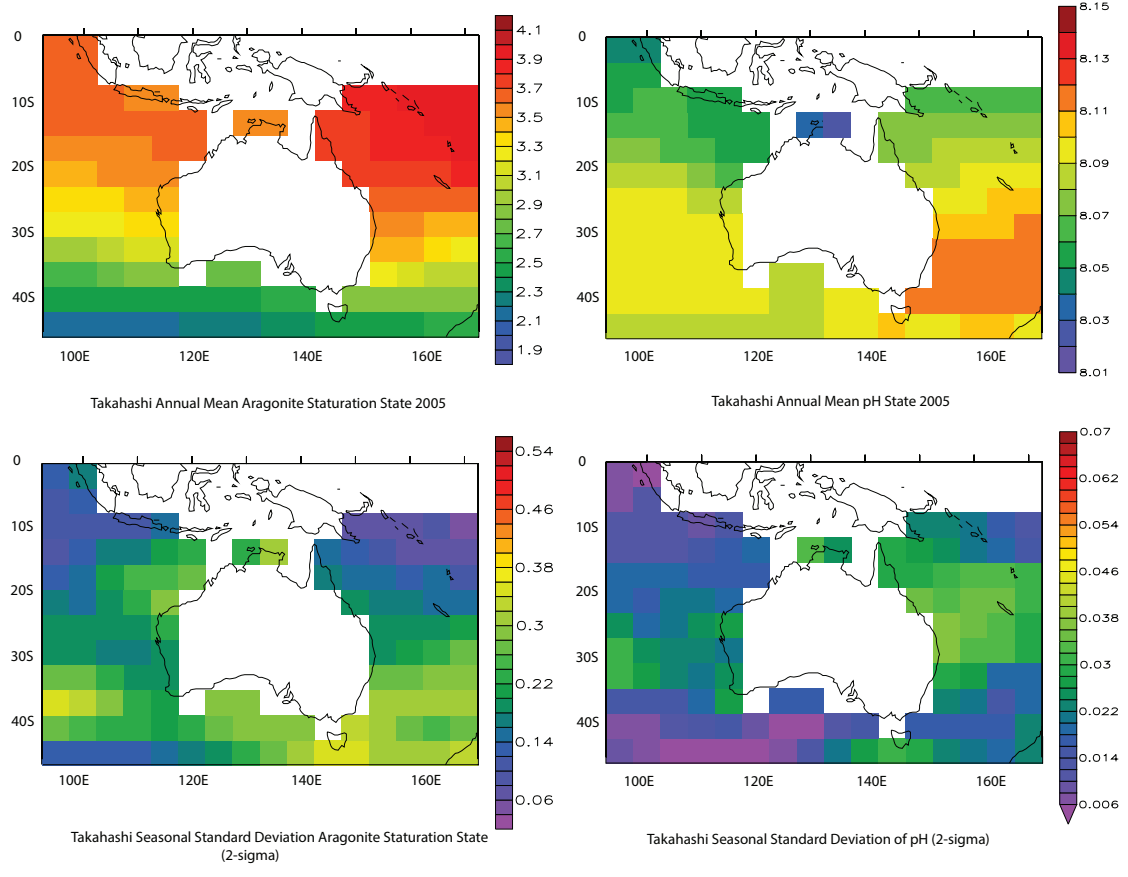
704 Figure 4 Comparison of aragonite saturation state (Ω_{AR}) from the observations at the

705 IMOS National Research Stations with the reconstructed values.



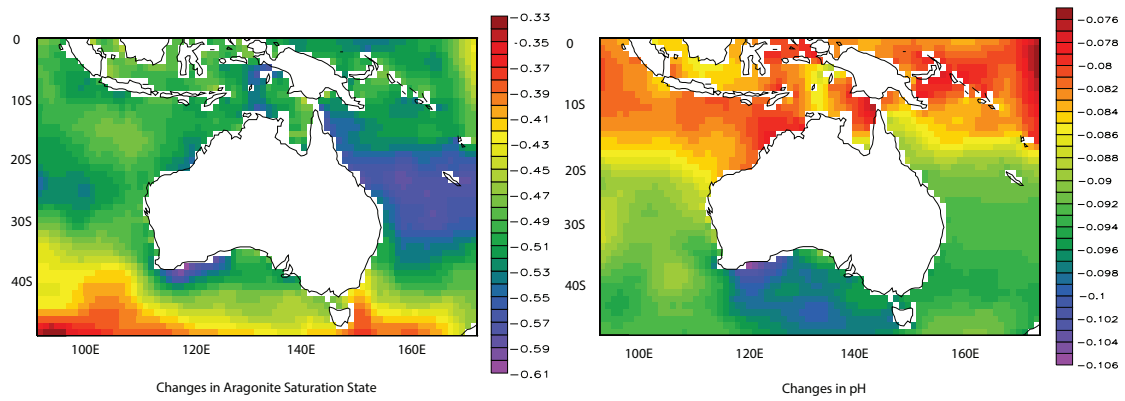
706
 707
 708
 709
 710
 711
 712
 713

Figure 5 Upper: the reconstructed annual mean aragonite saturation state and pH for the period 2000-2009; Lower: the seasonal variability given by 2 times the standard deviation ($2\text{-}\sigma$) of the seasonal variability in aragonite saturation state and pH from the period 2000-2009.



714
 715
 716
 717
 718
 719
 720
 721
 722
 723
 724
 725

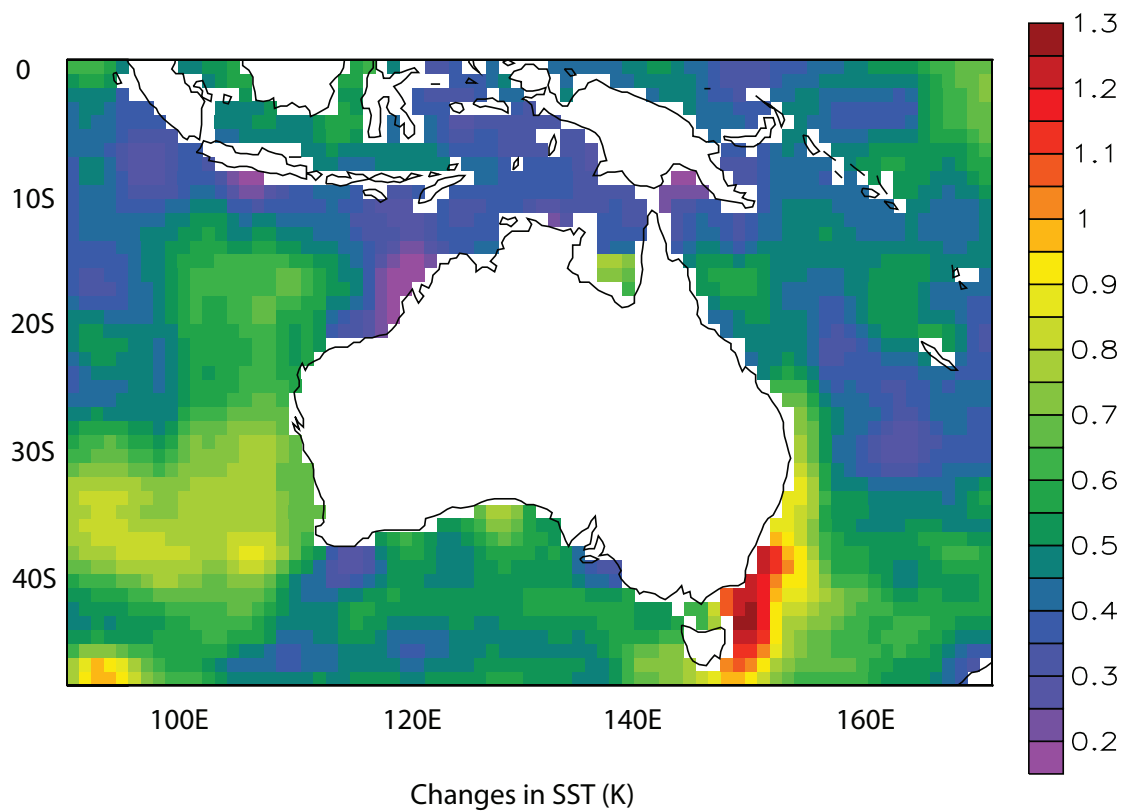
Figure 6 Upper: the annual mean aragonite saturation state and pH for 2005 from Takahashi et al (2014); Lower: standard deviation (2σ) of the seasonal variability in aragonite saturation state and pH for 2005 from Takahashi et al (2014).



726

727

728 Figure 7 Annual mean 120-year differences (2000-2009 and 1880-1889) in aragonite
 729 saturation state and pH.

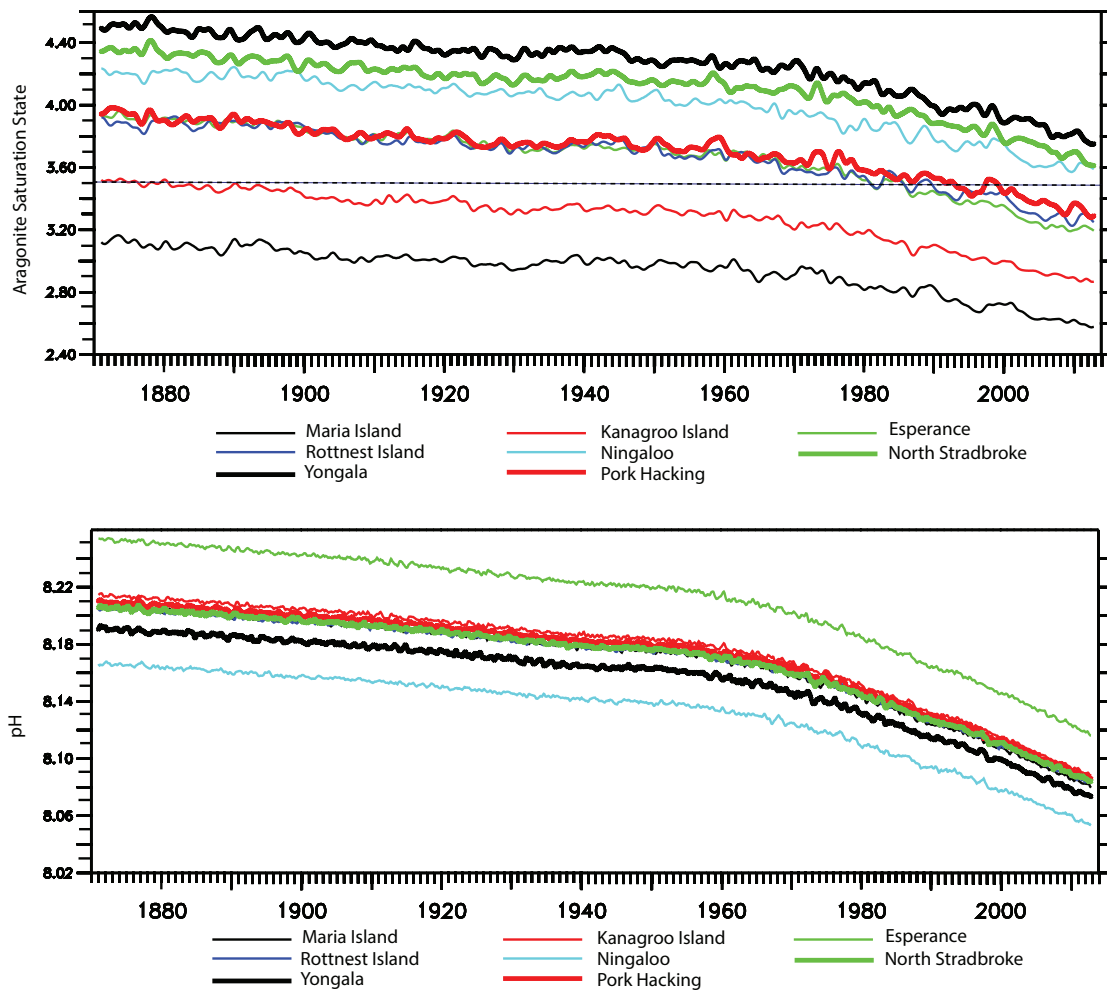


730

731

732 Figure 8 Annual mean 120-year differences (2000-2009 and 1880-1889) in SST.

733



734
 735
 736
 737
 738
 739
 740
 741
 742
 743
 744
 745
 746
 747
 748
 749

Figure 9 Reconstructed time series of annual mean aragonite saturation state (upper) and pH (lower) at the IMOS-NRSs. Overlain on the upper plot is the threshold for the transition to marginal conditions for coral reefs (3.5) from Guinotte et al. (2003)

Voyage ¹	Region/Expocode	Latitude	Longitude	Period	Number
Section P13	West Pacific 31VIC92_0_1_2	0°S - 5°S	164°E - 165°E	Oct 1992	13
Section P10	West Pacific 3250TN026/1	0°S - 5°S	145°E - 146°E	Oct 1993	11
Section P21	Coral Sea 318M19940327	17°S - 25°S	155°E - 170°E	Jun 1994	49
Section P9	West Pacific 49RY9407_1	0°S - 3°S	142°E - 143°E	Aug 1994	7
FLUPAC	West Pacific 35A319940923	0°S - 15°S	165°E - 167°E	Sep 1994 - Oct 1994	66
Section I8S/I9S	Indian Ocean 316N145_5	32°S - 45°S	95°E - 115°E	Dec 1994 - Jan 1995	29
Section I9N	Indian Ocean 316N145_6	0°S - 32°S	93°E - 106°E	Jan 1995 - Feb 1995	100
Section SR3	Southern Ocean AR9404_1	44°S - 45°S	146°E - 147°E	Jan 1995 - Feb 1995	5
Section I8N/I5E	Indian Ocean 316N145_7	31°S - 34°S	91°E - 115°E	Apr 1995	57
Section I3	Indian Ocean 316N145_8	20°S - 22°S	90°E - 114°E	Apr 1995 - May 1995	31
Section	West Pacific 49HG19950414	1°S - 35°S	153°E - 163°E	Apr 1995 - May 1995	25
Section I4	Indian Ocean 3175MB95_07	31°S - 43°S	90°E - 110°E	Sep 1995 - Oct 1995	28
Section I10	Indian Ocean 316N145_13	9°S - 25°S	106°E - 112°E	Nov 1995	76
Section I2	Indian Ocean 316N145_14_15	8°S - 9°S	90°E - 106°E	Dec 1995	37
Section SR3	Southern Ocean 09AR19960822	44°S - 45°S	146°E - 147°E	Sep 1996 - Oct 1996	5
Section I2	Indian Ocean 09AR20000927	28°S - 34°S	94°E - 115°E	Sep 2000 - Nov 2000	66
Section SR3	Southern Ocean 09AR20011029	44°S - 45°S	146°E - 147°E	Oct 2001	7
Section I5	Indian Ocean 74AB20020301	31°S - 35°S	91°E - 115°E	Apr 2002	34
OISO-10	Southern Ocean 35MF20030123	45°S	146°E	Jan 2003	5
Section P6W	West Pacific 49NZ20030803	30°S	154°E - 170°E	Aug 2003	40
Section I3	Indian Ocean 49NZ20031209	20°S - 22°S	90°E - 113°E	Jan 2004	33
Section I9S	Southern Ocean I09S_09AR20041	35°S - 44°S	115°E	Dec 2004	18
Section P10	West Pacific 49NZ20050525	0°S - 4°S	145°E - 146°E	Jun 2005	18
TransFuture5	Tasman Sea/ Coral Sea	10°S - 40°S	144°E - 172°E	Feb 2007 - Sep 2011	1460
Section I8S	Indian Ocean I08S_33RR20070	28°S - 45°S	94°E - 95°E	Mar 2007	79
Section I9N	Indian Ocean I09N_33RR20070	0°S - 28°S	93°E - 95°E	Mar 2007 - Apr 2007	103
Section I5	Indian Ocean I05_33RR200903	31°S - 35°S	90°E - 115°E	Apr 2009 - May 2009	128
Section P21	West Pacific 49NZ20090521	18°S - 25°S	154°E - 170°E	Jun 2009	52
Section P6W	West Pacific	30°S	154°E -	Nov 2009 -	93

	318M20091121		170°E	Dec 2009	
SS201004	Indian Ocean	21°S - 23°S	112°E - 115°E	May 2010	92
Total					2772

750

¹ <http://cdiac.ornl.gov/ftp/oceans/>

751

752 Table 1. Cruise data used to derive the salinity versus total alkalinity relationship for
753 surface waters in Australian regional seas.

754

755

756

757

758

759

760

761

762

763

764

765

766

767

768

769

770

771

772

773

774

775

776

777

778

779

780

781
 782
 783
 784

	Lat	Lon	SST - <i>BIAS</i>	SST - <i>R</i>	OmA - <i>BIAS</i>	OmA <i>-R</i>	n
Esperance	33° 56S	121° 51E	0.8	0.93	0.09	-0.06	16
Kangaroo Island	35° 49S	136° 27E	0.38	0.84	0.01	0.03	27
Maria Is	42° 36	148° 14E	0.6	0.93	0.07	0.83	40
Rottneest Is	32° 25S	115° 25S	1.01	0.92	0.06	0.26	33
Ningaloo	21° 52S	113° 57S	0.08	0.95	0.17	0.62	11
Yongala	19° 19S	147° 27S	0.13	0.94	0.27	0.45	37
Port Hacking	34° 5S	151° 6S	0.82	0.89	0.09	0.58	46
North Stradbroke	27° 18S	153° 6S	0.08	0.96	0.06	0.78	40

785
 786
 787
 788
 789
 790
 791
 792
 793
 794
 795
 796
 797

Table 2: The locations of the NRS sites used in this study, along with the biases, correlation coefficient (*R*) between the SST and aragonite saturation state observed at the site with values from our reconstruction, HadSST and calculated omega, respectively. Also listed are the number of observations used in calculating the Biases and Correlations